# Investigating cubane formation and effect of co-crystallization agents in oxo-bridged Co complexes using X-ray absorption spectroscopy

A. Gaur[1,2*], Deepa Sharma[3], N. Nitin Nair[4], B. K. Mehta[3], B. D. Shrivastava[4], Monsumi Gogoi[5], Nirupamjit Sarmah[5], B. K. Das[5]

[1]*Institute for Chemical Technology and Polymer Chemistry, Karlsruhe Institute of Technology (KIT), Engesserstrasse 20, D-76131 Karlsruhe, Germany*
[2]*Institute of Catalysis Research and Technology, Karlsruhe Institute of Technology (KIT), Karlsruhe, D-76131 (Germany)*
[3]*School of Studies in Chemistry and Bio-chemistry, Vikram University, Ujjain 456010, India*
[4]*School of Studies in Physics, Vikram University, Ujjain 456010, India*
[5]*Department of Chemistry, Gauhati University, Guwahati 781 014, India*

*Corresponding author: abhijeet.gaur@kit.edu, abhijeetgaur9@gmail.com*

## Abstract

The formation of cubane core and effect of co-crystallization agent have been studied in the oxo-bridged Co complexes using X-ray absorption spectroscopy. XAFS at Co K-edge have been measured in the oxo-bridged Co complexes $[Co_4O_4(O_2CCH_3)_4(C_5H_5N)_4]$(**1**), **1**.$0.5NaNO_3·8H_2O$(**2**), **1**.$NaClO_4·3.5H_2O$(**3**) and $[Co_4O_4(O_2CCH_3)_4(NH_3)_4]$(**4**). Complexes **2** and **3** actually contain the same complex **1** co-crystalized by $NaNO_3$ and $NaClO_4$ moieties. While **1** and **4** are in powder form, **2** and **3** are in crystalline form. Different XANES features have been correlated to the coordination around the absorbing Co atom in all the complexes. EXAFS analysis has been performed to determine coordination environment around the Co atoms to confirm the formation of the oxo-cubane structure in these complexes. For each of the Co centers present at the four different positions of the cubane core in complexes **2** and **3,** XANES spectra have been theoretically simulated and simultaneously p-DOS calculated to examine the effect of co-crystallizing moieties interactions with the individual Co centres present in these two complexes. After preliminary indication by EXAFS analysis, XANES simulations were also performed to examine the presence of defect dicubane structure in **4.** The study can be helpful in the detection of these structures during in-situ/operando studies of these catalytically active complexes.

Keywords – Cubane; Co-oxo complexes; X-ray absoption near edge structure; Extended X-ray absorption fine structure; Ab initio calculations; Density of states

## 1. Introduction

Transition metal coordination compounds and complexes have various applications. One of the important applications is as catalyst in different reactions e.g., in oxidation of organic compounds. In most of the homogeneous processes using transition metal salts and complexes as catalytic systems, separation and recovery of catalyst is difficult. Hence, efforts have been directed towards finding heterogeneous catalysts. In the recent past, cubane like clusters of $Co^{3+}$ have been developed, which have been found to display good heterogeneous activity. First example of $[Co_4(\mu_3-O_4)]^{4+}$ cubane core was reported by Dimitrou et. al[1]. Cyclic voltammetric examination of the cubane core cobalt complex showed one-electron reversible oxidation vs. ferrocene[2]. Beattie et. al[3] isolated neutral pyridine containing cobalt(III) acetate cubane from solution of cobalt(III) acetate in methanol after addition of pyridine and also by two other methods using cobalt(II) acetate and characterized the cubane by single crystal X-ray diffraction. The structure of the symmetric neutral cubane $[Co_4(\mu_3-O)_4(\mu-CH_3CO_2)_4(C_5H_5N)_4]$ (**1**) was reported to have each of the four $Co^{3+}$ and four $O^{2-}$ ions present at the alternate corners of an approximate cube, which forms the core of the complex. The oxide anions act as $\mu_3$-briging ligands and the pyridine ligands occupy the most outlying sites of the octahedral Co(III) centres and stabilise the +3 oxidation state of cobalt to facilitate the formation of the complex. Fig. 1 shows the labelled molecular structure of cubane core present in complex **2**.
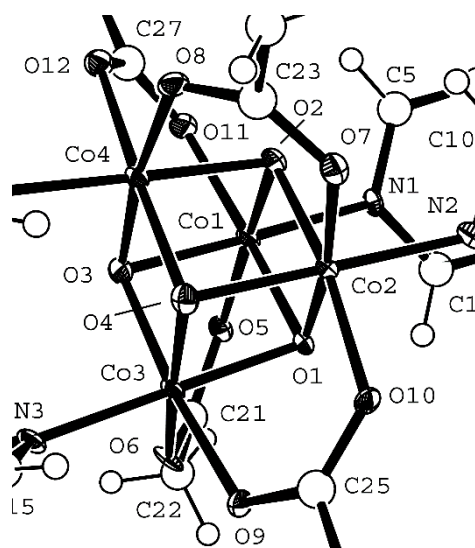


Fig. 1. A labelled molecular structure representation (ORTEP) of the cubane core present in complex **2** as determined by crystallography[4].

Several cobalt(III) cubane like complexes of the type $Co_4O_4(O_2CR)L_4$, where R is methyl or an aryl group and L = py  have been synthesized  and their applications as catalyst

have been studied in various oxidation reactions by Das *et al*[5]. The complex with R = $C_6H_5$ and L = (4-CNpy) has been used as a catalyst for the homogeneous air oxidation of α-pinene under atmospheric pressure and found to yield α-pinene oxide with verbenol and verbenone as the other products, with high selectivity for α-pinene oxide[6]. The same complex was immobilized on organomodified hexagonal mesoporous silica support and used as catalyst in aerobic oxidation of α-pinene. The catalyst proved to be heterogeneous and found to give best reported combination of activity and selectivity to epoxide[7]. Another tetrameric cubane complex with R = $CH_3$ and L = (4-CNpy) was used as catalyst in the oxidation of *p*-xylene to *p*-toluic acid[8]. Complex **1**, immobilised on a porous organomodified silica has been used as an efficient heterogeneous catalyst for the highly selective oxidation of benzylic alcohols and cyclohexanols using tert-butyl hydroperoxide (TBHP) as oxidants[4]. The catalyst remains reusable without any significant loss of activity in the process.

The electrochemical behavior of the oxo-cubane complexes, prepared by using R = $CH_3$ and L = py (complex **1**), 4-Mepy, 4-Etpy and 4-CNpy[9], indicated that $[(Co^{III})_4(\mu_3\text{-}O)_4]^{4+}$ core present in the complexes undergoes a reversible one-electron oxidation to $[(Co^{III})_3Co^{IV}(\mu_3\text{-}O)_4]^{5+}$ core at potential < 1V (employing Ag/AgCl as the reference electrode) which suggest the suitability of these complexes for the oxidation of organic compounds. Complex **1** was found to be useful in aerobic oxidation of neat ethylbenzene and *p*-xylene[10].

Another important application of the molecular $Co_4O_4$ cubane complex **1** is in catalyzing efficient water oxidizing activity when powered by a standard photochemical oxidation source or electrochemical oxidation[11]. The catalytic water oxidation activity of the complex has been found to be comparable with several other homogeneous water oxidation catalysts. It is also possible to couple this complex to a photosensitizer for light induced water oxidation[12]. Development of efficient water oxidation catalysts made from earth-abundant materials for the oxygen evolving half reaction is expected be useful in the technology needed for creation of solar fuels derived from renewable foodstock[12].

Looking at the catalytic importance of these oxo-cubane complexes of cobalt, it was considered important to probe the finer details of the local environment of Co(III) cubane like core present in oxo-carboxylate cobalt clusters using X-ray absorption spectroscopy (XAS) as the catalytic activity of these materials is highly correlated to their electronic structure. XAS is one of the important characterization techniques used to investigate local and molecular properties of the absorbing metal atoms in these metal-oxo complexes[13] which include oxidation state, metal–ligand distance, structural distortions and the degree of disorder[13-14].

The Co complexes studied are $Co_4O_4(O_2CCH_3)_4(py)_4$(**1**), $Co_4O_4(O_2CCH_3)_4(py)_4 \cdot$ $0.5NaNO_3 \cdot 8H_2O$(**2**), $Co_4O_4(O_2CCH_3)_4(py)_4 \cdot NaClO_4 \cdot 3.5H_2O$(**3**) and $Co_4O_4(O_2CCH_3)_4(NH_3)_4$ (**4**). The complexes are of the type $Co_4O_4(O_2CR)_4L_4$. With R = CH_3 and L = py, the complex is $Co_4O_4(O_2CCH_3)_4(py)_4$(**1**) and with R = CH_3 and L = NH_3 it is $Co_4O_4(O_2CCH_3)_4(NH_3)_4$(**4**). Complex **1,** which is simply $Co_4O_4(O_2CCH_3)_4(py)_4$ (**1**), obtained in powder form.[1] Complex **1** with co-crystallising agents $0.5NaNO_3.8H_2O$ and $NaClO_4.3.5H_2O$ has the compositions $Co_4O_4(O_2CCH_3)_4(py)_4 \cdot 0.5NaNO_3 \cdot 8H_2O$(**2**) and $Co_4O_4(O_2CCH_3)_4(py)_4 \cdot$ $NaClO_4 \cdot 3.5H_2O$(**3**), obtained in crystalline form. In complexes **2** and **3**, the cubane-like Co(III)-oxo complex, i.e., **1** remains connected in the crystal lattice through weak interactions to the co-crystallizing moieties, i.e., $NaNO_3$ and $NaClO_4$. These interactions can modulate the electronic structure of the complex to some extent and thus electron density around the $Co^{3+}$ ions present in the cubane core in the two crystalline forms of the complex may be somewhat different.

In the present study the formation of cubane structure in these Co-oxo complexes is probed by combination of XANES (X-ray absorption near edge structure) fingerprinting, EXAFS (extended X-ray absorption fine structure) analysis and theoretical XANES simulations to establish the spectroscopic nature of the cubane structure in general. Though formation of cubane has already been established using X-ray crystallography[5] for crystalline forms **2** and **3** but the interaction of the co-crystallisation agents can affect the cubane structure of Co core present in powder form **1** which can be studied using XANES combined with the structural parameters determined from EXAFS. On the other hand, **4** is the complex where ligand pyridine has been replaced by NH_3 and its crystal structure is still to be determined. Thus, it will be interesting to study the coordination environment of Co atoms in this complex to probe whether oxo-cubane structure was formed or not. Intensity and shape of some characteristic XANES features can give an estimate of distortion present in the sample. Using the crystallographic data obtained with the complexes having co-crystallization agents $0.5NaNO_3 \cdot 8H_2O$ and $NaClO_4 \cdot 3.5H_2O$, ab-initio XANES simulations have been performed separately for each of the Co metal centers present at the four corners of the cubane. Specific features observed in the calculated XANES spectra at four different positions of Co centers have been correlated with the variation in p-density of states (DOS) in order to compare their electronic structures.

## 2. Experimental and Data analysis

The complexes studied have been synthesized by using standard preparation methods and characterized by various spectroscopic and other analytical techniques[5, 9]. XAS

measurements were performed at the CAT-ACT beamline (energy range 3.5 - 50 keV) at the KIT synchrotron light source[15]. CAT-ACT´s superconducting multipole wiggler and a double crystal monochromator Si(111) provide high intensity (flux ~ $5\times10^{10}$ photons/s/100 mA) and an energy resolution $E/\Delta E > 1\times10^4$ at the Co K-edge energy (~7709 eV). For calibration purpose, XAS spectra of Co metal foil were recorded simultaneously with samples and the first inflection point in the derivative spectrum of Co foil was assigned the value of ~ 7709 eV. For recording X-ray absorption spectra of the four Co complexes, absorption screens were prepared in the form of pellets from calculated amount of finely powdered samples to yield an edge step of ~1.0 across the Co K-edge (~ 7709 eV) for the sample with total absorption length less than $2.5^{16}$. Thus, it is important that the sample should be uniform, and the thickness should be optimized to produce a high-quality absorption signal in transmission mode. The calculated amount of sample is mixed with a cellulose (binder) and then by using a mortar and pestle the mixture is reduced to a fine powder to make sure that it is completely homogenous. XAS spectra of references compounds $CoO$ and $Co_2O_3$ were also measured for XANES fingerprinting purpose.

EXAFS data analysis was performed using the software packages *Athena* and *Artemis*[17]. The program *Athena* was first used to process the raw data (absorption coefficient µ(E) as function of photon energy E by subtracting a smooth background from the data. The spectrum is normalized by regressing a linear function to the pre-edge region (-150 to -30 eV before the edge energy) and by regressing a linear or quadratic function to the post-edge region (50‑1000 eV above the edge energy). Normalized spectra are produced by subtracting the pre-edge line from the entire data spectrum and then dividing the spectrum by the step height[16]. Normalized µ(E) spectra are then converted to χ(k) spectra which are then Fourier transformed into R-space. Fitting of the EXAFS data was performed using the *Artemis* program by generating theoretical models from available crystallographic data[5] . The models were fitted to the experimental data in k- space and R-space to determine energy shifts ($\Delta E_0$) and structural parameters, including changes in the path length ($\Delta R$), passive electron reduction factor ($S_0^2$), coordination number (N) and relative mean-square displacement of the atoms (Debye-Waller factor, $\sigma^2$).

Ab-initio XANES calculations which include real-space full multiple scattering approach and the *l*-density of state (DOS) calculations (where *l* is orbital angular momentum) have been performed for the complexes by using computer code *FEFF9*[18]. *FEFF9* provides the angular momentum projected electron density of states between the defined photon energy range. This module is particularly useful for examining the densities of states which will be

helpful in interpretation of XANES. In the present study as we are studying the Co K-edge XANES and the origin of XANES features are closely related to the metal 4p density of states (DOS), thus $p$-DOS have been calculated simultaneously. For calculations in *FEFF9*, the input file has been generated by utilizing the available crystal structure data for the complexes by running the ATOMS module available in the *IFEFFIT* package[17]. In the present ab-initio calculations, Hedine-Lundqvist potential was chosen and XANES, SCF (Self-Consistent Field), FMS (Full Multiple Scattering) and Absolute cards were used[19]. In FEFF9, the energy dependent exchange correlation potential to be used for the fine structure and the atomic background can be specified. The calculated potential can be corrected by adding a constant shift to the Fermi level which is typicaly of the order of 1 eV and in most of the cases, the Hedin-Lundqvist self-energy is appeared to be the optimal choice. The self-consistent potential (SCF) parameters were as follows: rfms = 4, lfms1 = 0, nscmt = 100, ca = 0.2, nmix = 1. The XANES parameters were as follows: xkmax = 4, xkstep = 0.07, vixan = 0. The LDOS card was added for density of states calculation with an energy range of -20 to 30 eV with a Lorentzian broadening with half-width of 0.1 eV.

## 3. Results and discussions

### 3.1 XANES interpretation

XANES spectra at the Co K-edge of studied complexes **1-4** along with the reference compounds CoO and $Co_2O_3$ are shown in Fig. 2(a). Characteristic XANES features observed in the complexes are discussed as follow -

**Chemical shift -** It can be observed from the figure that, as expected, the K absorption edge of $Co_2O_3$ is found to be shifted to the higher energy as compared to that of CoO due to presence of Co in higher oxidation state, i.e., +3 in $Co_2O_3$. For the studied complexes **1-3**, the shift in the absorption edge with respect to the Co elemental edge (~7709 eV) is of the same order as that of $Co_2O_3$ showing the presence of $Co^{3+}$ in these complexes. The edge of complex **4** lies more closer to CoO than $Co_2O_3$. Hence, the values of edge shift (chemical shift) indicates the higher presence of $Co^{2+}$ as well as $Co^{3+}$ ions in complex **4**, i.e., mixed valence nature of this complex.

**Pre-edge peak -** The pre-edge peak P has been shown more clearly in Fig. 2(b). It can be observed that the spectra of complexes **1-3** show a clear pre-edge peak in the region 7709-7711 eV. This peak is attributed to the 1s-3d transition and is observed with weak intensity in

octahedral Co(III) compounds[20-21]. The intensity of peak in **3** is comparatively higher as compared to **1** and **2** and is quite weak in compound **4.**
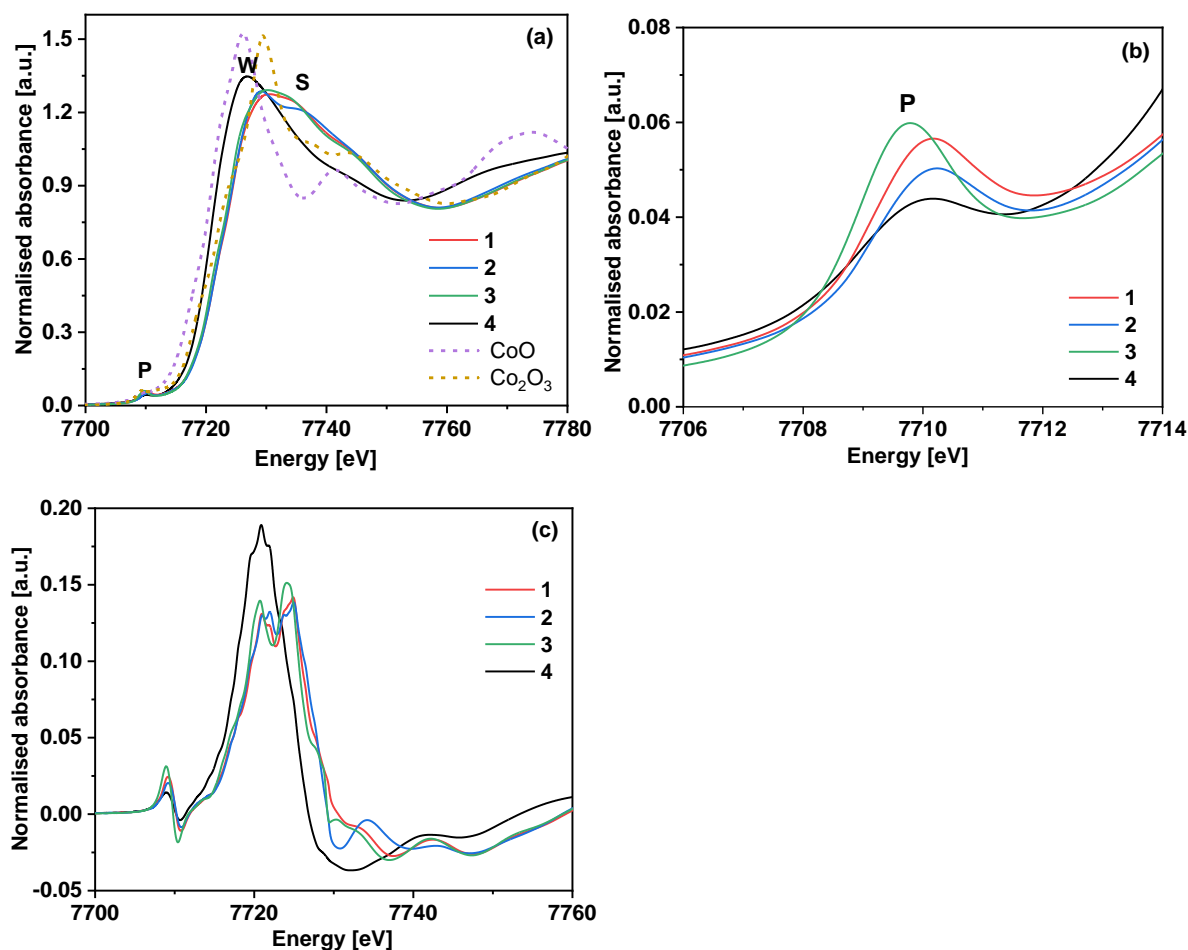


Fig. 2. For complexes **1-4** (a) Co K-edge XANES spectra for the complexes along with the references CoO and $Co_2O_3$. (b) Pre-edge peak P, shown enlarged, c) Corresponding derivative XANES spectra.

The higher intensity of the pre-edge peak shows distortion in centrosymmetric nature of octahedral coordination. As mentioned earlier **2** and **3** actually contain **1** but crystalized in different co-crystallization moieties, $NaNO_3$ and $NaClO_4$. Thus, in **3** comparatively strong interaction with $NaClO_4$ increases the distortion in octahedral coordination of Co which on the other hand is weak for $NaNO_3$ as indicated by the lower intensity of P in **2** as compared to **3**. Thus, different co-crystallization moieties can alter the electronic structure of the complex in distinctive manner. The high pre-edge intensity is also correlated to the oxidation state as in higher oxidation states there is shortening of the metal–oxygen distances which results in increased mixing between the p and d orbitals. In case of **4,** very low pre-edge peak at

comparatively lower energy has been observed. Hence, presence of Co in relatively lower oxidation in **4** can also be observed from pre-edge peak.

**White line -** As reported earlier $Co^{3+}$ XANES spectra exhibit the white line peak W at 7727 eV and a neighbouring peak at around ~ 7736 eV[20]. Both of these peaks have been assigned to the transitions from cobalt 1s orbital to molecular orbitals, mainly the 4p orbitals. Complexes **1-3** exhibit such peaks at ~7729 eV and 7736.2 eV indicating presence of Co in +3. However, complex **4** shows only a single peak at 7726 eV and no neighboring peaks. The white line peak shifts to lower energy with decrease in effective nuclear charge on the nucleus[14, 20] indicating presence of mixed $Co^{3+}/Co^{2+}$ ions in **4**. Regarding the intensity of this peak, complexes **1-3** show similar intensity but complex **4** shows higher intensity.

Another feature S, in the form of hump is observed above the white line in complexes **1-3** which is correlated to the multiple scattering from relatively heavy backscatterer atoms[21]. It point towards the presence of heavy Co backscatterers around the absorbing Co atom in these complexes. Such a shoulder is absent in complex **4**, indicating that the absorbing Co atom may be coordinated majorly to weak scatters like oxygen/ nitrogen and less Co atoms.

**Post-edge minima -** A post-edge minima is observed in Co(II) complexes in the energy range 7749.3-7750.3 and in Co(III) complexes in the range 7757.5-7761.6 eV[22]. In the present work, the complexes **1-3** have post-edge minima at around 7758.6 eV indicating $Co^{3+}$ nature of centers in these complexes. In complex **4**, the minima is at 7752.6 eV pointing towards a mixed nature $Co^{3+}/Co^{2+}$ of centers.

**Derivative spectra –** Fig. 2(c) shows the derivative of XANES spectra of the complexes. In the complexes **1-3**, the main Co-K absorption edge, i.e., the rising part in the absorption spectra (Fig. 1(a)) is found to split into two edges. This splitting can be clearly seen in the derivative spectra Ffig.1(c)) as two peaks. For complexes **1-3**, the presence of the two peaks in the derivative spectra with slightly higher intensity for **3** shows that Co centers in these complexes have identical coordination environment, i.e., cubane structure. In the complex **4**, the edge part does not split and hence in the derivative spectra a single peak is observed. This also confirms that the electronic structure and coordination of Co centers in **4** is different from that in complexes **1-3**.

Thus, based on the XANES characteristics, it can be concluded that **1**, **2** and **3** have Co in 3+ oxidation state and the coordination environment around Co centers is also identical in these complexes supporting presence of cubane structure. The XANES features observed for **1-3** are also similar to those reported by Nguyen et al.[11] where complex **1** and five other

8

$Co_4O_4$ based complexes, synthesized from **1** using different organic linkers, have been studied using XAS. However, it has been observed in the present study that the interaction with co-crystallization moieties increases distortion in **3** as compared to **1** and **2**. On the other hand XANES indicate presence of mixed valent Co centers, i.e., $Co^{2+}/Co^{3+}$ in **4** with distinct coordination environment in higher metal shells than other studied complexes.

### 3.2 EXAFS analysis -

$k^3$ weighted $\chi(k)$ spectra for the four complexes **1-4** are shown in Fig. 3(a). EXAFS oscillations for the complexes **1-3** are similar to each other indicating presence of identical local environment around absorbing Co atom in these complexes. The oscillations in complex **4** are comparatively weak and shifted to lower k values showing presence of Co with different local environment. The corresponding Fourier transformed spectra are shown in Fig. 3(b) where as expected amplitude and position of the backscattering peaks are found to be similar for complexes **1-3**. In **4**, the backscattering peaks are obtained at almost the same position but with almost half the amplitude of the peaks in complexes **1-3**. Further information can be obtained by fitting EXAFS with the corresponding theoretical model.
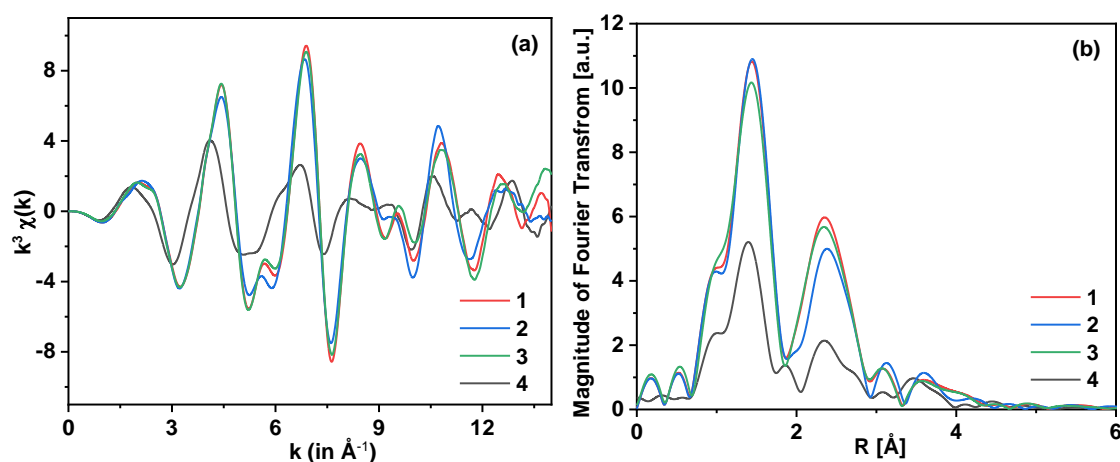


Fig. 3 (a)- $k^3$ weighted $\chi(k)$ vs. k spectra of the complexes **1-4**, (b) Corresponding Fourier transformed spectra in R-space

EXAFS analysis has been performed using program *Artemis* to extract the structural parameter for complexes **1-4**. The crystallographic data[5] of **2** obtained by crystalizing **1** with $NaNO_3$ have been used to generate theoretical model, which has been fitted to the experimental data of the complexes in R-space in the range of 1.0 – 4 Å as well as in k-space in the k-range of 2.4 - 12.5 Å$^{-1}$ using k weight of 3. EXAFS fitting in R-space along with contribution from different paths for complexes **1-4** are given in Figs. 4(a-d) respectively. The structural parameters obtained from fitting are given in Table 1.

Table 1. Structural parameters obtained from EXAFS fitting. N = coordination number, R = Bond distance by XAS, $R_c$ = Bond distance by crystallography[5], $\sigma^2$ = Debye-Waller factor (bracket shows the error bar). *R factor* is goodness of fit parameter.

| | Complex **1** | | | Complex **4** | | | Complex **2** | | | | Complex **3** | | | |
|---|---|---|---|---|---|---|---|---|---|---|---|---|---|---|
| | $S_0^2$ = 0.98, | | | $S_0^2$ = 0.91, | | | $S_0^2$ = 0.97, | | | | $S_0^2$ = 0.98, | | | |
| | $\Delta E_0$ = 1.9 (0.7) | | | $\Delta E_0$ = 2.1(0.3) | | | $\Delta E_0$ = 2.2 (0.1) | | | | $\Delta E_0$ = 1.8 (0.7) | | | |
| | *R factor* = 0.000351 | | | *R factor* = 0.00201 | | | *R factor* = 0.00026 | | | | *R factor* = 0.00055 | | | |
| | N | R (Å) | $\sigma^2 \times 10^3$ (Å²) | N | R (Å) | $\sigma^2 \times 10^3$ (Å²) | N | R (Å) | $R_c$ (Å) | $\sigma^2 \times 10^3$ (Å²) | N | R (Å) | $R_c$ (Å) | $\sigma^2 \times 10^3$ (Å²) |
| O2 | 1 | 1.85 | 4.9(3.8) | 1 | 2.04 | 7.7(2.9) | 1 | 1.86 | 1.84 | 8.0(8.4) | 1 | 1.84 | 1.86 | 5.7(2.5) |
| O1 | 1 | 1.88 | 4.9(3.8) | 1 | 2.07 | 7.7(2.9) | 1 | 1.88 | 1.87 | 8.0(8.4) | 1 | 1.85 | 1.87 | 5.7(2.5) |
| O3 | 1 | 1.90 | 4.9(3.8) | 1 | 2.08 | 7.7(2.9) | 1 | 1.90 | 1.88 | 8.0(8.4) | 1 | 1.85 | 1.87 | 5.7(2.5) |
| O5 | 1 | 1.92 | 5.0(4.7) | 1 | 1.90 | 4.8(1.8) | 1 | 1.90 | 1.95 | 3.3(1.4) | 1 | 1.92 | 1.95 | 3.0(1.5) |
| O11 | 1 | 1.93 | 5.0(4.7) | 1 | 1.90 | 4.8(1.8) | 1 | 1.91 | 1.95 | 3.3(1.4) | 1 | 1.93 | 1.96 | 3.0(1.5) |
| N1 | 1 | 1.92 | 5.0(4.7) | 1 | 1.90 | 4.8(1.8) | 1 | 1.91 | 1.95 | 3.3(1.4) | 1 | 1.94 | 1.97 | 3.0(1.5) |
| Co3 | 1 | 2.70 | 5.3(3.5) | | - | | 1 | 2.74 | 2.70 | 7.8(2.5) | 1 | 2.69 | 2.71 | 4.2(1.2) |
| Co4 | 1 | 2.70 | 5.3(3.5) | | - | | 1 | 2.74 | 2.70 | 7.8(2.5) | 1 | 2.70 | 2.71 | 4.2(1.2) |
| Co2 | 1 | 2.81 | 5.3(3.5) | 1 | 2.81 | 6.3(1.5) | 1 | 2.84 | 2.80 | 7.8(2.5) | 1 | 2.81 | 2.82 | 4.2(1.2) |

The results given in the table 1 confirm octahedral coordination around Co atom in all the complexes. In complex **1-3**, six O/N atoms are observed at distances in the range ~ 1.84-1.94 Å around the absorbing Co atom. Also, presence of 3 neighbouring Co atoms has been observed at distances in the range ~ 2.70-2.84 Å. In case of complexes 2 and 3, the values of bond distances obtained from crystallography[5] are also given in the table for comparison with the corresponding bond distances obtained from EXAFS. Thus, it can be observed that EXAFS results agree well with the reported crystallographic results[5] which confirms formation of the cubane structure in these complexes where each of the four $Co^{3+}$ and four $O^{2-}$ ions are present at the alternate corners of an approximate cube.

In case of complex **4**, six O/N atoms constituting the octahedra around the absorbing Co atom are observed at somewhat longer distances in the range ~ 1.90-2.08 Å, and only one Co backscatterer was observed at 2.81 Å. Such longer Co-O/N bonds forming the octahedra around Co ion have reported in case of formation of a defect dicubane core with two missing vertexes[23-24]. Also, in this complex presence of only one neighbouring Co indicate that the cubane-like $[Co_4(\mu\text{-}O)_4]$ structure is not complete. Thus, formation of defect dicubane core in **4** can be the possible reason for its distinct spectroscopic behavior in XANES as well as EXAFS.
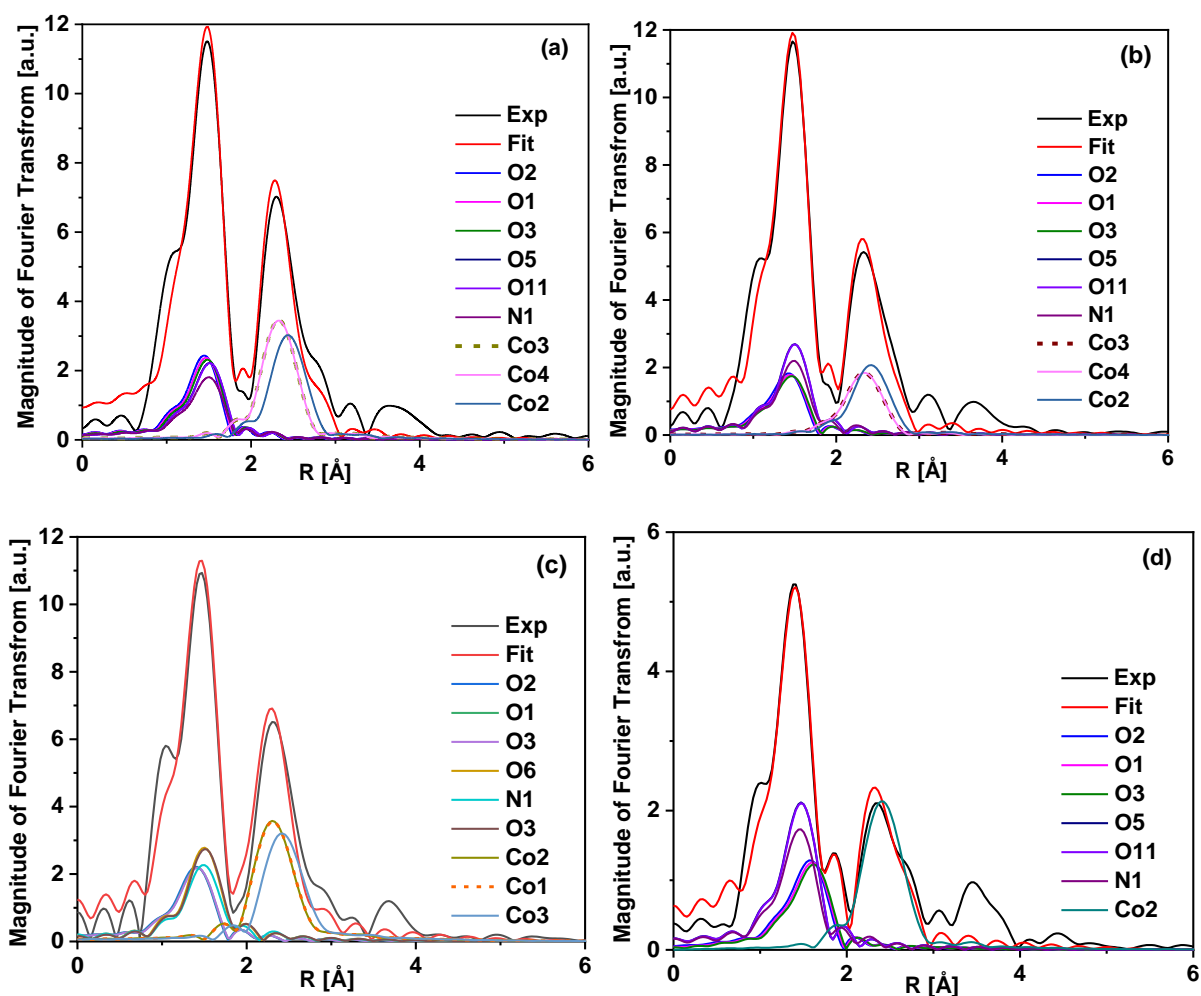
Fig. 4 - EXAFS fittings for the four complexes **1-4** in R-space. The experimental curve (black line) and the theoretical fit (red line) along with contributions of different paths are shown in the figures. Figs.(a)-(d) correspond to complexes **1-4** respectively.

In order to further investigate the presence of cubane core as well as defect dicubane core in these complexes, XANES simulations have been performed as discussed in section 3.3.

## 3.3 Ab-initio XANES calculations

### 3.3.1 Cubane

Cubane structure present in **1** is shown in Fig. 5. It consists of four each of $Co^{3+}$ (pink spheres) and $O^{2-}$ ions (red spheres) occurring at alternate corners of a cube. The metal centres adopt nearly octahedral six-coordinate geometries where Co-O/N bond lengths are in the narrow ranges of 1.86 - 1.96 Å[5]. On the other hand, the four Co atoms form an approximate tetrahedron with Co...Co separations of ~ 2.75 Å.
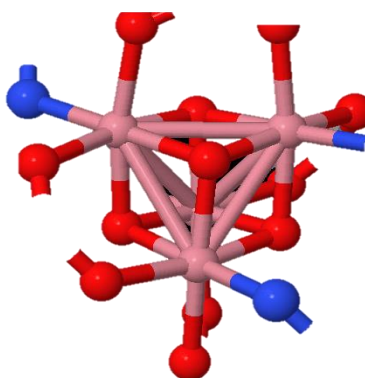
Fig. 5 - Structure of cubane core in the Co oxo-cubane complex. Co (pink spheres) and O (red spheres)

As mentioned in the introduction, crystal structure of complex **1** has been determined from two different crystals of complex containing **1** in the compositions **1**.0.5NaNO$_3$.8H$_2$O (**2**) and **1**.NaClO$_4$.3.5H$_2$O (**3**). In these crystallite forms **2** and **3**, some weak interactions with the co-crystallizing moieties NaNO$_3$ and NaClO$_4$ can modulate the electronic structure of the complexes to some extent and thus the electron density around the Co$^{3+}$ ions in the complexes **2** and **3** may be somewhat different. To investigate this behavior of Co ions in these complexes, ab-initio XANES calculations have been performed using program *FEFF9*. Separate calculations have been done for each of the Co ions present at the four different corners of the cubane in the two complexes as shown in Fig. 5. The crystallographic data[5] determined from the crystals of complexes **2** and **3**, having different compositions, have been used to generate the feff.inp fies for XANES simulations. This has been done to observe if the interaction with different co-crystallization agents can affect the electronic structure at the four Co centers, which can be observed by the differences in their XANES features. As the origin of these features are closely related to the Co 4p density of states (DOS), hence, the p-DOS have been calculated simultaneously to observe the change in it for the Co metal ion present at the four positions.

Fig. 6(a) shows the simulated XANES spectra for the Co centres forming the cubane structure present in **2** along with its experimental XANES spectra. XANES simulations has been done by setting the core hole at the four different positions, namely, Co1, Co2, Co3 and Co4 for Co centres present in the cubane structure to compare their electronic structure. The corresponding p-DOS curves are shown in the Fig. 6(b).
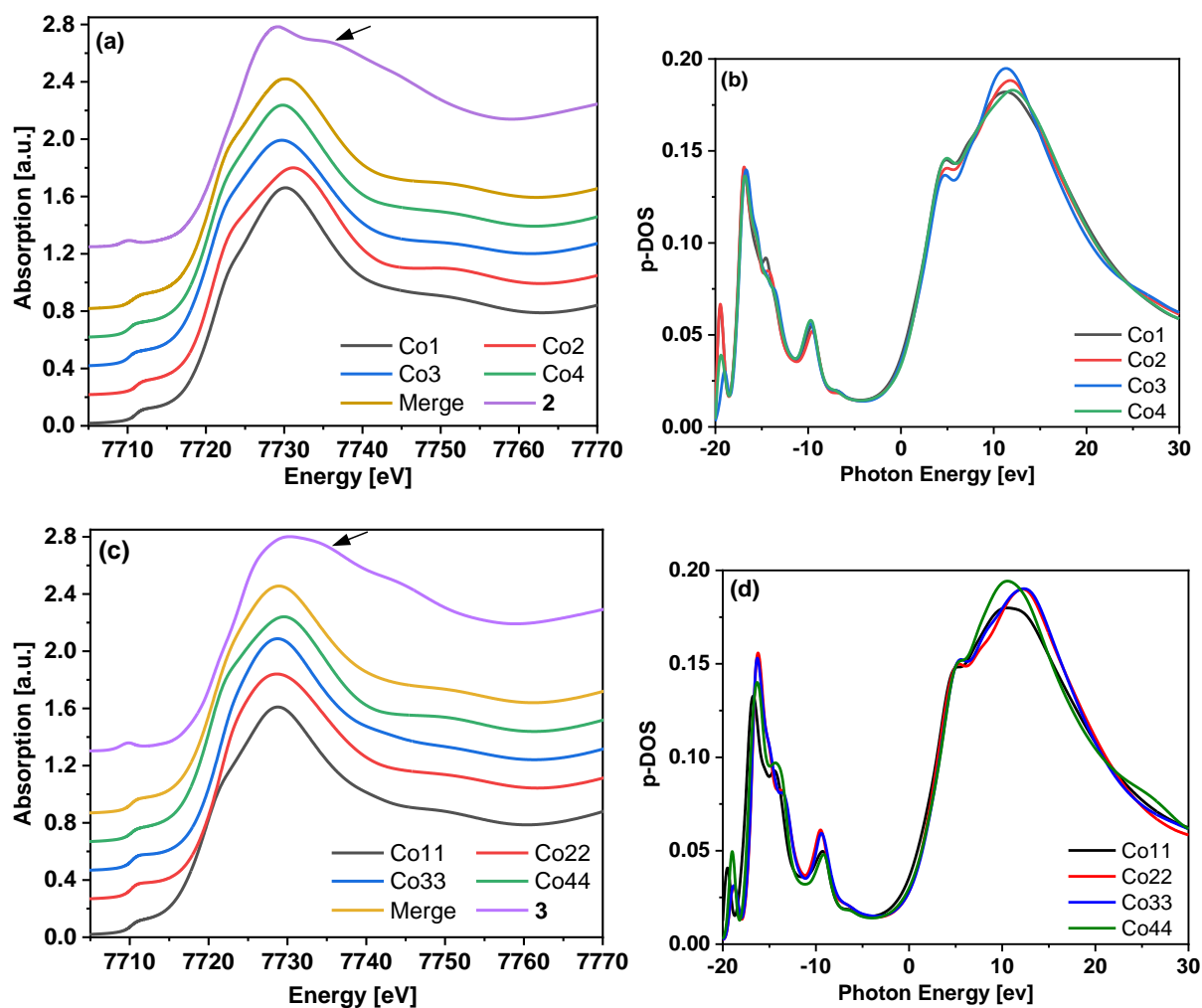
Fig.6 - (a) Simulated XANES spectra for the four Co centres Co1, Co2, Co3 and Co4 forming the cubane structure in **2** along with its experimental XANES spectra and (b) Corresponding p-DOS. (c) Simulated XANES spectra for the four Co centres Co11, Co22, Co33 and Co44 forming the cubane structure in **3** along with its experimental XANES spectra and (d) Corresponding p-DOS. In Figs. (a) and (c), the curves are vertically displaced for clarity.

As shown in Fig. 6(a), in the pre-edge region a weak peak has been observed in the case of all the four Co centres indicating their similar oxidation state of +3 and distorted octahedral coordination. The white line maxima for Co2 position has been observed at comparatively higher energy than other three Co positions indicating slightly higher charge on metal ion at this position. In the edge part, Co1, Co3 and Co4 centres show a mild shoulder while Co2 shows comparatively strong shoulder. This can be attributed to the strong interaction of metal with ligands at position Co2 leading to higher distortion. In the metal K-edge spectra of some 3d transition metal complexes, a shoulder is observed in the main edge region. This shoulder is due to metal localized 1s→4p transition with "shakedown" contribution arising from a coupled ligand to metal charge transfer (LMCT) transition. It has been observed that this transition is sensitive to the nature of metal ligation and depends on

13

the axial position[25]. Thus, presence of axial ligation in such complexes gives rise to this weak shoulder. For octahedral coordination, presence of this shoulder indicates deviation of metal centre from the six coordinated geometry and also that significant amount of distortion is present.

In the corresponding p-DOS shown in Fig. 6(b), the maxima has been observed at same position for Co1, Co3 and Co4 with amplitude for Co1 slightly higher than others. For Co2, the p-DOS maxima has been observed to be shifted towards higher energy which is in correspondence with the occurrence of its white line maxima at higher energy. After white line, the experimental spectra of the complex **2** shows a hump (marked by arrow) which is not observed in any of simulated XANES spectra of four Co centers. This hump has already been discussed in *Section 3.1*. This can be is correlated to the multiple scattering from relatively heavy backscatterer atoms[21] and point towards the presence of heavy Co backscatterers around the absorbing Co atom in these complexes. Remaining post-edge region has been found to be similar for the four Co centres and the corresponding merged spectrum, also shown in the figure, has spectral shape in agreement with the experimental spectrum.

Similar XANES simulated spectra for the four Co centres Co11, Co22, Co33 and Co44 present in the cubane structure in **3** are shown in Fig. 6(c) along with its experimental spectrum. In this case also, a weak peak has been observed in the pre-edge region for all the Co centres indicating their oxidation state of +3 and distorted octahedral coordination. The white line maxima for Co44 position has been observed at comparatively higher energy than other three Co positions indicating slightly higher charge on metal ion at this position. In the edge part, Co11 and Co44 centres show a shoulder while Co22 and Co33 centres have smooth edge region indicating comparatively strong interaction with ligands at the positions Co11 and Co44. This strong interaction has been supported from the corresponding p-DOS shown in Fig. 6(d) where comparatively broad distribution of density of states have been observed for Co centre at Co11. The p-DOS maxima for Co22 and Co33 has been observed at higher energy as compare to its position in Co11 and Co44, though the amplitude of maxima is highest for Co44. In the post-edge part, the experimental spectra of the complex **3** also shows a hump (marked by arrow) similar to that in complex **2** which is not observed in any of simulated XANES spectra of the four Co centres. Remaining post-edge region has been found to be similar for the four Co centres and the corresponding merged spectrum has spectral shape in agreement with the experimental spectrum.

To summarize for NaNO$_3$ (**2**), it has been found that the electronic behavior of Co atoms present at the different positions of a cubane-like geometry is almost same at three

positions Co1, Co3 and Co4 while for position Co2 higher interaction with ligands has been observed. Similarly, in case of $NaClO_4$ (**3**), comparatively higher interaction has been observed for Co centers present at positions Co11 and Co44 as compared to positions Co22 and Co33 of the cubane. Thus, by using XANES simulations interactions of Co-oxo centers with the co-crystallizing salts, i.e., $NaNO_3$ and $NaClO_4$ moieties can be observed in the two crystalline forms.

### 3.3.2 **Defective cubane**

As reported in literature[23-24], there is possibility of formation of defect cubane core which can strongly change the nature of Co centers present in these Co-oxo complexes. Thus, in order to investigate the electronic structure of Co centers forming such defective cubane core and their corresponding density of states, XANES simulations has been done using the recently reported crystal structure of mixed valent defect dicubane complex[23].
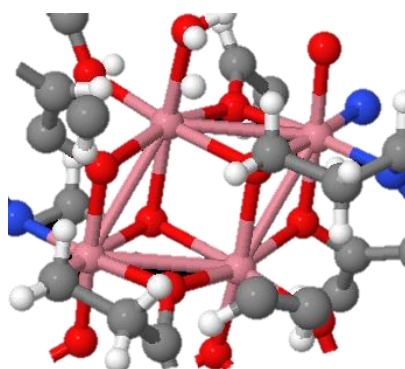


Fig. 7. Structure of defect cubane core in the mixed valent dicubane complex. Co (pink spheres) and O (red spheres)

Defect dicubane structure with two missing vertices is shown in Fig. 7. Distorted octahedral geometry has been observed for all the cobalt ions with different coordination environments. As reported, two cobalt ions D Co1 and D Co3 exhibit identical N2O4 environments and the remaining D Co2 and D Co4 display O6 environments. The shorter Co-O bond lengths for D Co1 and D Co3 as compared to that for D Co2 and D Co4 indicates that former are in a higher oxidation state (+3) than later (+2) which is also supported by bond valence sum analysis[23].
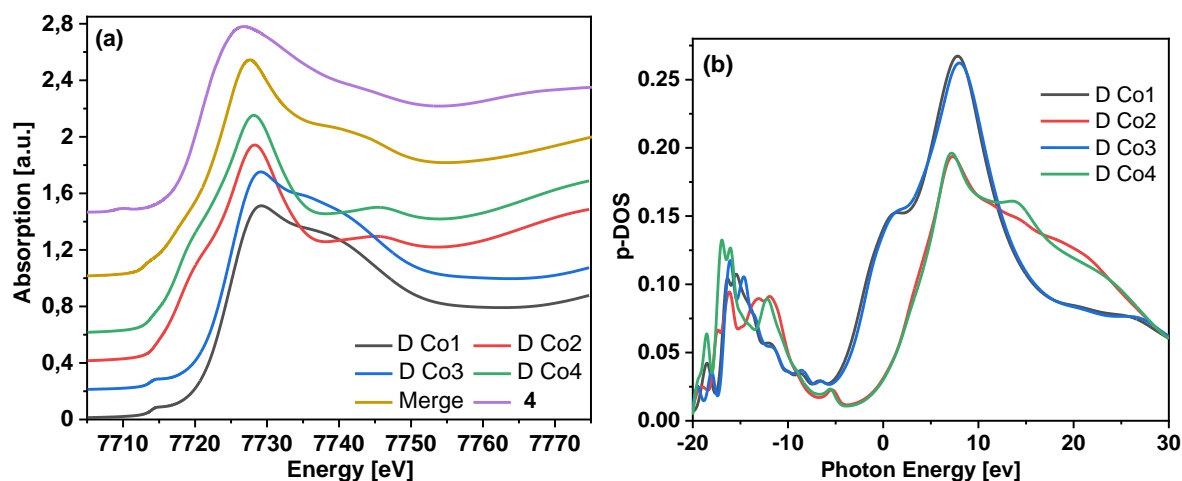
Fig. 8 - (a) Simulated XANES spectra for the four Co centres present in the defect cubane structure along with the experimental XANES spectra of **4** and (b) Corresponding p-DOS.

Simulated XANES spectra for the four Co centers are shown in Fig. 8(a) and the different features observed are discussed as follows. The edge shift for D Co1 and D Co3 have been observed to be high as compared to that for D Co2 and D Co4 indicating presence of Co in higher oxidation state at these positions. D Co1 and D Co3 show pre-edge peak which is characteristic of Co in +3 state, however such peak is not observed in case of D Co2 and D Co4. In the corresponding p-DOS shown in Fig 8(b), for D Co1 and D Co3, splitting of the p-DOS (two maxima) has been observed in the edge region due to increased intermixing between the p and d orbitals whereas for D Co2 and D Co4 smooth increase in p-DOS has been observed in this energy region. Higher intensity of white line has been observed for D Co2 and D Co4 as compared to that for D Co1 and D Co3. From these differences in XANES region, it has been confirmed that that Co ions present at positions D Co1 and D Co3 have oxidation state of +3+ and those present the positions D Co2 and D Co4 have +2 state.

In Fig. 8(a), the merged spectrum, obtained from the spectra of four Co centers present in the defect dicubane core is compared with that of experimental spectrum of **4**. Nice agreement between the spectral shape of the **4** and that of merged spectrum has been observed indicating possible presence of defect dicubane structure in this complex. Thus, results obtained from XANES simulations are in accordance with the EXAFS fitting results which indicate that cubane structure is not complete in **4**.

This result, however, is not in line with the earlier findings for the complexes $Co_4O_4(O_2CCH_3)_4(NH_3)_4$ and $Co_4O_4(O_2CC_6H_4-4-X)_4(NH_3)_4$ with X = H, CH$_3$, OCH$_3$, NO$_2$, Cl), all of which showed ESI-MS and ^{1}H NMR data supporting the cubane-like geometry of the tetrameric Co$^{3+}$ clusters present in these complexes[26]. The elemental analysis, ESI-MS and ^{1}H NMR data for the complex **4** are given in supplementary information. The possible reason

for this disagreement can be as follows. It can be observed from the $^1$H NMR spectrum of complex **4** that there is no indication of the presence of Co$^{2+}$ in the native sample because that would have broadened / shifted the spectral signals. However, as the measurements are done in solution-state, there is a slight possibility that the native solid sample contains Co$^{2+}$ but it was oxidized to Co$^{3+}$ when it was dissolved into the solvent. As $^1$H NMR spectra with sharp signals have been the hallmark of a range of diamagnetic species of the type [Co$_4$O$_4$(O$_2$CR)$_4$(L)$_4$], hence, the magnetic susceptibility and ESR (Electron Spin Resonance) spectrum of the complexes are not measured. Further, despite the minor deviations of the experimental values from the theoretical values of C, H, N content it is believed that the $^1$H NMR and the ESI-MS results provide convincing proof of purity of the sample. However, the confirmation of mixed Co valence states (Co$^{3+}$ as well as Co$^{2+}$) in complex **4** from the present XAS studies which are solid-state measurements conflicts with the diamagnetic $^1$H NMR spectral results done in solution-state. Though there is no indication of interaction of X-ray beam with the samples during present XAS measurements, but that possibility can also be examined in future experiments. In view of this, exhaustive spectroscopic studies including XAS, $^1$H NMR, ESR and magnetic susceptibility measurements on the entire series of complexes analogous to **4** will be planned in future for obtaining detailed information on chemical nature and electronic structure of these cobalt complexes having NH$_3$ as ligands.

## 4. Conclusions

Cubane formation in Co-oxo complexes has been studied using XANES as well as EXAFS to establish the spectroscopic nature of the cubane structure in general. Different XANES features showed presence of octahedrally coordinated Co$^{3+}$ ions in complexes **1-3**. Comparatively higher intensity of pre-edge peak in **3** as compared to **1** and **2** indicated high distortion in octahedral structure of Co due to strong interaction with NaClO$_4$. EXAFS analysis confirmed that in **1-3**, Co centers have octahedral coordination with six O/N atoms in the range 1.84-1.94 Å along with 3 Co-Co backscattering contributions at ~ 2.80 Å which supports formation of cubane-like structure in these complexes. XANES simulation performed for the individual Co centers supports formation of cubane-like geometry in these complexes **1-3**, where different electron density around the Co$^{3+}$ ions confirm interaction with the co-crystallizing salts, i.e., NaNO$_3$ and NaClO$_4$ moieties.

In case of complex **4**, XANES features indicated presence mixed valence Co$^{2+}$ as well as Co$^{3+}$ ions. EXAFS analysis showed six O/N atoms constituting the octahedra are observed at higher distances in the range 1.90-2.08 Å, and only one Co backscatterer was found to be

present, suggesting that formation of cubane is not complete in **4**. Further, XANES simulation supports formation of defect dicubane structure in this complex with presence of $Co^{2+}/Co^{3+}$ ions which is in accordance with the EXAFS fitting and XANES fingerprinting results.

Thus, XAS analysis including XANES fingerprinting, EXAFS fitting together with theoretical XANES simulations are able to successfully detect the presence of cubane-like geometry in the studied complexes. The interaction with co-crystallizing agent is another important observation of this study which should be considered while making crystal of these complexes for determination of structure. Also, the formation of defect dicubane, i.e., incomplete cubane distinguished based on the XAS analysis can further help in the detection of such structures during in-situ/operando studies of these complexes having important application in the field of catalysis.

**Data Availability Statement**

The data that supports the findings of this study are available within the article.

# References

1.	Dimitrou, K.; Folting, K.; Streib, W. E.; Christou, G., Dimerization of the [Co2III(OH)2] core to the first example of a [Co4IIIO4] cubane: potential insights into photosynthetic water oxidation. *Journal of the American Chemical Society* **1993,** *115* (14), 6432-6433.

2.	Dimitrou, K.; Brown, A. D.; Concolino, T. E.; Rheingold, A. L.; Christou, G., Mixed-valence, tetranuclear cobalt(,) complexes: preparation and properties of [CoO(OCR)(bpy)] salts. *Chemical Communications* **2001,** (14), 1284-1285.

3.	Beattie, J. K.; Hambley, T. W.; Klepetko, J. A.; Masters, A. F.; Turner, P., The chemistry of cobalt acetate—IV. The isolation and crystal structure of the symmetric cubane, tetrakis[(μ-acetato)(μ3-oxo) (pyridine)cobalt(III)] · chloroform solvate, [Co4(μ3-O)4(μ-CH3CO2)4(C5H5N)in4] · 5CHCl3 and of the dicationic partial cubane, trimeric, [(μ-acetato)(acetato)tris(μ-hdyroxy(μ3-oxo) hexakispyridinetricobalt(III)]hexafluorophosphate · water solvate, [Co3(μ3-O)(μ-OH)3(μ-CH3CO2(CH3CO2(C5H5N)6[PF6]2 · 2H2O. *Polyhedron* **1998,** *17* (8), 1343-1354.

4.	Sarmah, P.; Chakrabarty, R.; Phukan, P.; Das, B. K., Selective oxidation of alcohols catalysed by a cubane-like Co(III) oxo cluster immobilised on porous organomodified silica. *Journal of Molecular Catalysis A: Chemical* **2007,** *268* (1), 36-44.

5.	Das, B. K.; Chakrabarty, R., Cobalt(III)-oxo cubane clusters as catalysts for oxidation of organic substrates. *Journal of Chemical Sciences* **2011,** *123* (2), 163-173.

6.	Chakrabarty, R.; Das, B. K., Epoxidation of α-pinene catalysed by tetrameric cobalt(III) complexes. *Journal of Molecular Catalysis A: Chemical* **2004,** *223* (1), 39-44.

7.	Chakrabarty, R.; Das, B. K.; Clark, J. H., Enhanced selectivity in green catalytic epoxidation using a supported cobalt complex. *Green Chemistry* **2007,** *9* (8), 845-848.

8.	Chakrabarty, R.; Kalita, D.; Das, B. K., Catalytic oxidation of p-xylene in water by cobalt(III) cubane cluster. *Polyhedron* **2007,** *26* (6), 1239-1244.

9.	Chakrabarty, R.; Bora, S. J.; Das, B. K., Synthesis, Structure, Spectral and Electrochemical Properties, and Catalytic Use of Cobalt(III)−Oxo Cubane Clusters. *Inorganic Chemistry* **2007,** *46* (22), 9450-9462.

10.	Chakrabarty, R.; Sarmah, P.; Saha, B.; Chakravorty, S.; Das, B. K., Catalytic Properties of Cobalt(III)−Oxo Cubanes in the TBHP Oxidation of Benzylic Alcohols. *Inorganic Chemistry* **2009,** *48* (14), 6371-6379.

11.	Nguyen, A. I.; Van Allsburg, K. M.; Terban, M. W.; Bajdich, M.; Oktawiec, J.; Amtawong, J.; Ziegler, M. S.; Dombrowski, J. P.; Lakshmi, K. V.; Drisdell, W. S.; Yano, J.; Billinge, S. J. L.; Tilley, T. D., Stabilization of reactive Co$_4$O$_4$ cubane oxygen-evolution catalysts within porous frameworks. *Proceedings of the National Academy of Sciences* **2019,** *116* (24), 11630-11639.

12.	Carrell, T. G.; Cohen, S.; Dismukes, G. C., Oxidative catalysis by Mn4O46+ cubane complexes. *Journal of Molecular Catalysis A: Chemical* **2002,** *187* (1), 3-15.

13.	van Oversteeg, C. H. M.; Doan, H. Q.; de Groot, F. M. F.; Cuk, T., In situ X-ray absorption spectroscopy of transition metal based water oxidation catalysts. *Chemical Society Reviews* **2017,** *46* (1), 102-125.

14.	Risch, M.; Klingan, K.; Ringleb, F.; Chernev, P.; Zaharieva, I.; Fischer, A.; Dau, H., Water Oxidation by Electrodeposited Cobalt Oxides—Role of Anions and Redox-Inert Cations in Structure and Function of the Amorphous Catalyst. *ChemSusChem* **2012,** *5* (3), 542-549.

15.	Zimina, A.; Dardenne, K.; Denecke, M. A.; Doronkin, D. E.; Huttel, E.; Lichtenberg, H.; Mangold, S.; Pruessmann, T.; Rothe, J.; Spangenberg, T.; Steininger, R.; Vitova, T.; Geckeis, H.; Grunwaldt, J.-D., CAT-ACT—A new highly versatile x-ray spectroscopy beamline for catalysis and radionuclide science at the KIT synchrotron light facility ANKA. *Review of Scientific Instruments* **2017,** *88* (11), 113113.

16.	Gaur, A.; Shrivastava, B. D.; Nigam, H. L., X-Ray Absorption Fine Structure (XAFS) Spectroscopy – A Review. *Proc Indian Natn Sci Acad* **2013,** *79* (4), 921-966.

17.	Ravel, B.; Newville, M., ATHENA, ARTEMIS, HEPHAESTUS: data analysis for X-ray absorption spectroscopy using IFEFFIT. *Journal of Synchrotron Radiation* **2005,** *12* (4), 537-541.

18.	Rehr, J. J.; Kas, J. J.; Vila, F. D.; Prange, M. P.; Jorissen, K., Parameter-free calculations of X-ray spectra with FEFF9. *Physical Chemistry Chemical Physics* **2010,** *12* (21), 5503-5513.

19.     FEFF    9.6.4    User's    Guide.    http://monalisa.phys.washington.edu/feffproject-feff-documentation.html.

20.     Adak, S.; Hartl, M.; Daemen, L.; Fohtung, E.; Nakotte, H., Study of oxidation states of the transition metals in a series of Prussian blue analogs using x-ray absorption near edge structure (XANES) spectroscopy. *Journal of Electron Spectroscopy and Related Phenomena* **2017,** *214*, 8-19.

21.     Gaur, A.; Nitin Nair, N.; Shrivastava, B. D.; Das, B. K.; Chakrabortty, M.; Jha, S. N.; Bhattacharyya, D., Study of distorted octahedral structure in 3d transition metal complexes using XAFS. *Chemical Physics Letters* **2018,** *692*, 382-387.

22.     Hall, M. D.; Underwood, C. K.; Failes, T. W.; Foran, G. J.; Hambley, T. W., Using XANES to Monitor the Oxidation State of Cobalt Complexes. *Australian Journal of Chemistry* **2007,** *60* (3), 180-183.

23.     Coban, M. B.; Gungor, E.; Kara, H.; Baisch, U.; Acar, Y., New mixed valence defect dicubane cobalt(II)/cobalt(III) complex: Synthesis, crystal structure, photoluminescence and magnetic properties. *Journal of Molecular Structure* **2018,** *1154*, 579-586.

24.     Ansari, I. A.; Sama, F.; Shahid, M.; Khalid, M.; Sharma, P. K.; Ahmad, M.; Siddiqi, Z. A., Synthesis, Spectral Characterization, X-ray and Magnetic Studies of Oxo-bridged Tetranuclear Coordination Polymers of Cobalt. *Journal of Inorganic and Organometallic Polymers and Materials* **2016,** *26* (1), 178-189.

25.     Chen, Y.; Wang, H.; Li, J.; Lockard, J. V., In situ spectroscopy studies of CO2 adsorption in a dually functionalized microporous metal–organic framework. *Journal of Materials Chemistry A* **2015,** *3* (9), 4945-4953.

26.     Gogoi, M. Studies on the synthetic use and catalytic applications of transition metal carboxylate complexes. Ph.D. thesis, Gauhati University, 2017.

# Investigating cubane formation and effect of co-crystallization agents in oxo-bridged Co complexes using X-ray absorption spectroscopy

A.Gaur[1,2*], Deepa Sharma[3], N.Nitin Nair[4], B.K.Mehta[3], B.D.Shrivastava[4], Monsumi Gogoi[5], Nirupamjit Sarmah[5], B.K.Das[5]

[1]*Institute for Chemical Technology and Polymer Chemistry, Karlsruhe Institute of Technology (KIT), Engesserstrasse 20, D-76131 Karlsruhe, Germany*
[2]*Institute of Catalysis Research and Technology, Karlsruhe Institute of Technology (KIT), Karlsruhe, D-76131 (Germany)*
[3]*School of Studies in Chemistry and Bio-chemistry, Vikram University, Ujjain 456010, India*
[4]*School of Studies in Physics, Vikram University, Ujjain 456010, India*
[5]*Department of Chemistry, Gauhati University, Guwahati 781 014, India*

*\*Corresponding author: abhijeet.gaur@kit.edu, abhijeetgaur9@gmail.com*

Elemental analysis of complex **4**, i.e., [Co$_4$O$_4$(O$_2$CCH$_3$)$_4$(NH$_3$)$_4$]

Found: C, 15.04 %; H,3.36 %; N, 8.83 %; calc. for C$_8$H$_{24}$N$_4$O$_{12}$Co$_4$: C, 15.90 %; H, 3.98 %; N, 9.28 %

| Molecular formula | Calc. Molar mass (g/mol) | [M]$^+$ peak (m/z) |
|---|---|---|
| Co$_4$O$_4$(O$_2$CCH$_3$)$_4$(NH$_3$)$_4$ | 603.72 | 603.68 |
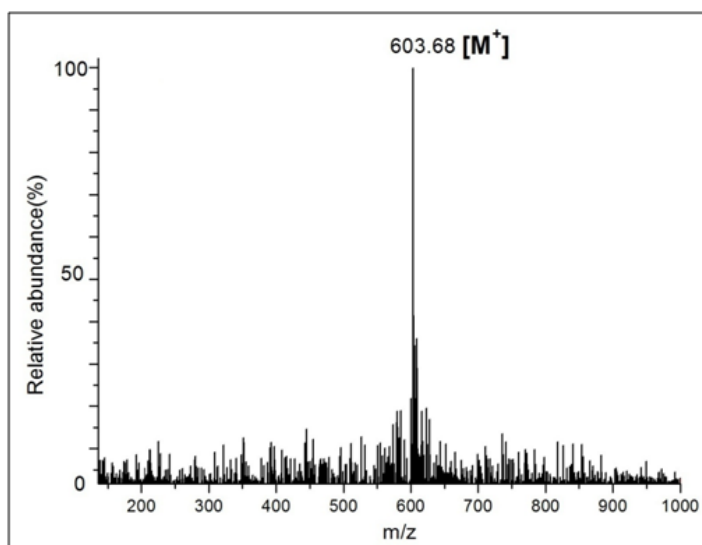


Figure S1. ESI-MS of Co$_4$($\mu_3$-O)$_4$($\mu$-O$_2$CMe)$_4$(NH$_3$)$_4$ in MeCN.
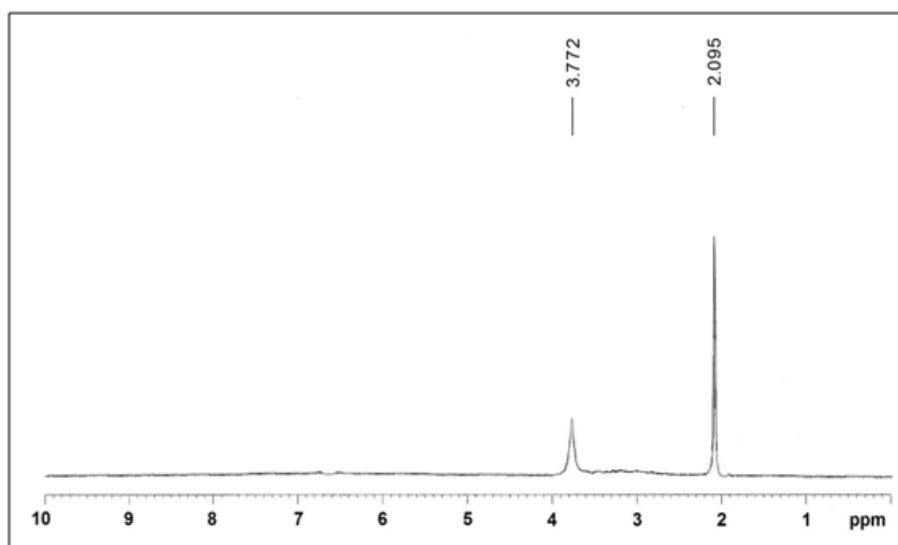


Figure S2. 400 MHz $^1$H-NMR spectrum of [Co$_4$($\mu_3$-O)$_4$($\mu$-O$_2$CMe)$_4$(NH$_3$)$_4$] in CDCl$_3$